Jacqueline A. Koehler,[1] Laurie L. Baggio,[1] Xiemin Cao,[1] Tahmid Abdulla,[1] Jonathan E. Campbell,[1] Thomas Secher,[2] Jacob Jelsing,[2] Brett Larsen,[1] and Daniel J. Drucker[1]

Glucagon-Like Peptide-1 Receptor Agonists Increase Pancreatic Mass by Induction of Protein Synthesis

Diabetes 2015;64:1046–1056 | DOI: 10.2337/db14-0883

Glucagon-like peptide-1 (GLP-1) controls glucose homeostasis by regulating secretion of insulin and glucagon through a single GLP-1 receptor (GLP-1R). GLP-1R agonists also increase pancreatic weight in some preclinical studies through poorly understood mechanisms. Here we demonstrate that the increase in pancreatic weight following activation of GLP-1R signaling in mice reflects an increase in acinar cell mass, without changes in ductal compartments or β-cell mass. GLP-1R agonists did not increase pancreatic DNA content or the number of Ki67$^+$ cells in the exocrine compartment; however, pancreatic protein content was increased in mice treated with exendin-4 or liraglutide. The increased pancreatic mass and protein content was independent of cholecystokinin receptors, associated with a rapid increase in S6 phosphorylation, and mediated through the GLP-1R. Rapamycin abrogated the GLP-1R–dependent increase in pancreatic mass but had no effect on the robust induction of *Reg3α* and *Reg3β* gene expression. Mass spectrometry analysis identified GLP-1R–dependent upregulation of Reg family members, as well as proteins important for translation and export, including Fam129a, eIF4a1, Wars, and Dmbt1. Hence, pharmacological GLP-1R activation induces protein synthesis, leading to increased pancreatic mass, independent of changes in DNA content or cell proliferation in mice.

Gut hormones secreted from specialized endocrine cells subserve multiple functions integrating control of food ingestion, gut motility, and the digestion, absorption, and assimilation of nutrients. The actions of enteroendocrine peptides to control lipid metabolism, body weight, and glucose homeostasis have engendered considerable translational interest given the increasing incidence of dyslipidemia, obesity, and diabetes. Glucagon-like peptide-1 (GLP-1), secreted from enteroendocrine L cells, reduces food intake, inhibits gastric emptying, and produces weight loss. GLP-1 also inhibits chylomicron secretion from enterocytes and lowers triglyceride levels in both preclinical and clinical studies (1). The most extensively studied action of GLP-1 is that of an incretin hormone, augmenting insulin and inhibiting glucagon secretion following meal ingestion, through actions targeting endocrine cells in the pancreas. Collectively, the glucoregulatory actions of incretin hormones led to the development of two distinct drug classes that lower glucose by potentiation of incretin action, dipeptidyl peptidase-4 (DPP-4) inhibitors and GLP-1 receptor (GLP-1R) agonists (2).

Although classical glucoregulatory actions of incretin-based therapies target the endocrine pancreas, the nonglycemic actions of GLP-1R agonists and DPP-4 inhibitors on the exocrine pancreas have received considerable attention (3). Spontaneous reports of pancreatitis in diabetic patients treated with incretin-based therapies stimulated interest in whether GLP-1R agonists affect the exocrine pancreas (4). Although results of preclinical studies are conflicting, the majority of experiments do not link activation of GLP-1R signaling to enhanced susceptibility to pancreatitis in rodents (4,5). Furthermore studies of transgenic reporter gene expression under the control of the endogenous murine *Glp1r* promoter (6) have not demonstrated GLP-1R expression in pancreatic acinarpt cells.

[1]Department of Medicine, Lunenfeld-Tanenbaum Research Institute, Mount Sinai Hospital, Toronto, Ontario, Canada
[2]Gubra, Hørsholm, Denmark
Corresponding author: Daniel J. Drucker, drucker@lunenfeld.ca.

Received 5 June 2014 and accepted 24 September 2014.

This article contains Supplementary Data online at http://diabetes.diabetesjournals.org/lookup/suppl/doi:10.2337/db14-0883/-/DC1.

Despite lack of evidence for GLP-1R expression in acinar cells of the rodent pancreas, several preclinical studies have demonstrated that GLP-1R agonists increase the mass of the pancreas, predominantly in mice (7,8) and in a subset of male nonhuman primates (9). Nevertheless, the increase in pancreatic weight following treatment with GLP-1R agonists has not been associated with histological abnormalities in the pancreas (3,9,10), and mechanistic explanations for changes in pancreatic mass have not been forthcoming. We show here that exendin-4 (Ex-4) and liraglutide increase pancreatic weight via induction of protein synthesis, without changes in acinar cell proliferation or DNA content. These actions were independent of receptors for cholecystokinin (CCK), required the classical *Glp1r*, and were abrogated by inhibition of the mammalian target of rapamycin (mTOR). Our findings provide an explanation for changes in pancreatic mass observed following treatment with GLP-1R agonists.

RESEARCH DESIGN AND METHODS

Reagents, Animals, and Treatments

Ex-4 was from CHI Scientific (Maynard, MA), liraglutide was from Novo Nordisk (Bagsværd, Denmark), and rapamycin (Rapamune) was from Wyeth (Montreal, Quebec). Peptides were dissolved in PBS (vehicle) and administered to mice by intraperitoneal injection (Ex-4, 10 nmol/kg, b.i.d.; or liraglutide, 75 μg/kg, b.i.d.). Rapamycin was diluted in 0.5% carboxymethacellulose (C4888; Sigma-Aldrich), 2.5% Tween-80. C57BL/6, *Cckar*$^{-/-}$, and *Cckbr*$^{-/-}$ mice were from The Jackson Laboratory (Bar Harbor, ME). Whole-body *Glp1r*$^{-/-}$ mice in the C57BL/6 background (11,12) and wild-type (WT) littermate control mice were generated by crossing *Glp1r*$^{+/-}$ mice. *Cckar*$^{-/-}$:*Cckbr*$^{-/-}$ (DKO) and WT littermate control mice were generated by crossing *Cckar*$^{+/-}$ and *Cckbr*$^{+/-}$ mice. Animal experiments were approved by the Animal Care Committee of the Mount Sinai Hospital.

Pancreatic Growth

Male C57BL/6 mice (8–10 weeks old) were administered exogenous Ex-4 or vehicle (PBS) for 7 days or 4 weeks. Male (not shown) and female *Cckbr*$^{-/-}$, *Cckar*$^{-/-}$ (7–12 weeks old), *Cckar:Cckbr*$^{-/-}$ (DKO) (8–13 weeks old), and WT littermate control mice were administered exogenous Ex-4 or vehicle for 10 days. Nonfasted mice were killed by CO_2 inhalation in the morning (~12 h after the last injection) unless otherwise indicated.

Time Course

Male C57BL/6 mice (11 weeks old) were injected with Ex-4 or vehicle every 12 h and pancreata were obtained at 4 h, 12 h, or 24 h to 7 days. For the 24-h to 7-day time points, mice were killed in the morning (~12 h after the last injection).

Rapamycin Study

Male C57BL/6 mice (8–10 weeks old) were administered vehicle (0.5% carboxymethacellulose, 2.5% Tween-80) or rapamycin (2 mg/kg 1 × daily i.p.) 30 min prior to the first (morning) injection of exogenous Ex-4 or PBS for 3 or 7 days.

High-Protein Diet Study

High-protein diet (HPD) (AIN-93M modified to contain 75% casein; D1206504) and control diet (CD) AIN-93M (D10012M) were from Research Diets (New Brunswick, NJ). *Glp1r*$^{-/-}$ and WT littermate control female mice (8–11 weeks old) were acclimatized to the CD for 1 week prior to being fed the HPD or CD ad libitum for 7 days.

Tissue Collection, Immunohistochemistry, and DNA/Protein and Water Content

Following euthanasia, mice were weighed, blood samples collected by cardiac puncture, and serum was stored at −80°C. The pancreas was removed, weighed, and cut in half lengthwise; one-half was fixed in 10% formalin for 24 h, the other half was cut into four equal sections from tail (attached to spleen) to head for RNA, protein, DNA/protein content, and water content. Immunohistochemistry and morphometry were done on 5-μm histological sections stained with hematoxylin and eosin or Ki67 (1:2,000, RM9106-S1; Thermo Scientific) by standard procedures. Sections were scanned and analyzed using the ScanScope CS system (Aperio Technologies) at 20× magnification. Immunohistochemistry for phospho-S6 ribosomal protein (Ser240/244, D68F8 XP; Cell Signaling) was performed according to the manufacturer's instructions. Immunohistochemistry for Reg3 (antisera, 1:200 dilution, Dr. Rolf Graf, University Hospital Zurich, Zurich, Switzerland) was performed using sodium citrate buffer pH 6.0 for antigen unmasking and overnight incubation with the Reg3 antibody. Edema was calculated following desiccation for 72 h and expressed as a percentage of wet weight (wet weight − dry weight/wet weight × 100). For analysis of DNA and protein content, pancreas samples were weighed, homogenized in a lysis buffer containing 0.1% Tx-100 and 5 mmol/L $MgCl_2$, and sonicated for 15 s. Protein content was measured using Bradford assay (Bio-Rad) and a Pierce BCA protein assay kit (Thermo Scientific), and DNA content was measured using a DNA quantification kit (DNAQF; Sigma-Aldrich).

Serum Amylase and Lipase Levels

Serum amylase activity was measured using the Phadebas Amylase Test (Magle Life Sciences, Cambridge, MA), and serum lipase activity was analyzed with the Lipase Color Assay (905-B; Sekisui Diagnostics, Charlottetown, PE, Canada). Serum amylase and lipase activity levels were also measured in serum samples from mice with secretagogue-induced pancreatitis induced by administration of five sequential hourly intraperitoneal injections of caerulein, 50 μg/kg body weight (8).

Quantitative Histological Analyses of Pancreas Mass

Stereological quantification of pancreas mass was carried out in collaboration with Gubra (Gubra ApS, Hørsholm, Denmark). Male C57BL/6 mice (12–13 weeks old) were administered exogenous Ex-4 (10 nmol/kg, b.i.d., i.p.),

liraglutide (75 μg/kg, b.i.d., i.p.), or vehicle for 14 days. Male *Glp1r*$^{+/+}$ and *Glp1r*$^{-/-}$ littermate controls (8–12 weeks old) were administered Ex-4 or vehicle for 14 days. Pancreata were removed en bloc in 4% formaldehyde and processed for stereological analyses as previously described (13). Ductal epithelial cells were detected with a rat anti-cytokeratin 19 antibody (ck19, 1:100; Hybridoma Bank, TROMA-III, University of Iowa, Iowa City, IA) and visualized with 3,3′-diaminobenzidine. β-Cells were detected with a guinea pig anti-insulin antibody (1:5,000, A0564; Dako) and visualized with NovaRED (Vector Laboratories). Non–β-cells were detected with an antibody cocktail consisting of rabbit anti-glucagon (1:5,000, H-028-02; Phoenix), rabbit anti-somatostatin (1:7,500, 0566; Dako), and rabbit anti-pancreatic polypeptide (1:5,000, B32-1; EuroProxima) and visualized with 3,3′-diaminobenzidine-nickel. Endocrine mass includes the combined mass of β-cells (mass of insulin immunoreactivity) and non–β-cells (mass of glucagon, somatostatin, and pancreatic polypeptide immunoreactivity) inside the islets.

Islet Isolation, RNA Extraction, and Quantitative Real-Time RT-PCR

Pancreatic islets were isolated as described previously (14) and incubated overnight in fresh RPMI (10% FBS, 100 units/mL penicillin, and 100 μg/mL streptomycin). The next morning, islets were handpicked for size and viability into 1.5-mL tubes. Total RNA from whole pancreatic tissue or islets was extracted using TRI Reagent (Sigma-Aldrich) and cDNA synthesis performed with random hexamers and SuperScript III (Invitrogen Canada). Quantitative real-time PCR was performed on an ABI PRISM 7900HT Sequence Detection System (Applied Biosystems, Foster City, CA) as previously described (8,14). Relative values for mRNA transcripts were normalized to the levels of cyclophilin (*Ppia*).

Western Blot Analysis

Whole-tissue extracts were prepared by homogenization in ice-cold RIPA buffer (1% nonidet P-40, 0.5% sodium deoxycholate, and 0.1% SDS in Tris-buffered saline) supplemented with protease and phosphatase inhibitors (Sigma-Aldrich), 5 mmol/L sodium fluoride, 5 mmol/L β-glycerophosphate, and 200 μmol/L sodium orthovanadate. The rabbit polyclonal antibodies phospho-p70 S6K (Thr389, 9205), phospho-eIF2a (Ser51, 9721), and phospho-S6 (Ser240/244, 2215) were from Cell Signaling Technologies (Beverly, MA) and used at a 1:1,000 dilution. 4EBP1 (BL895) was from Bethyl Laboratories Inc. (Montgomery, TX) and used at a 1:1,000 dilution, or HSP90 (610418; BD Biosciences) at a 1:2,000 dilution. Images were scanned using a Kodak Imager (4000 MM PRO; Kodak Imaging Station), and quantification was performed using Carestream Molecular Imaging software (standard edition V.5.0.2.30).

Proteomics

Preparation of pancreas samples for proteomics was performed as previously described using the filter-aided sample preparations II protocol (15). In brief, male C57BL/6 mice (8–10 weeks old) were administered exogenous Ex-4 or vehicle for 7 days (n = 5), and the pancreas was removed and homogenized in 4% SDS lysis buffer (4% SDS, 100 mmol/L Tris/HCl pH 7.6, 0.1 mol/L dithiothreitol) and incubated at 98°C for 3 min, followed by brief sonication and centrifugation (5 min, 16,000g). Equal protein (250 μg) was mixed with 200 μL UA buffer (8 mol/L urea in 0.1 mol/L Tris/HCl pH 8.5) and loaded onto Micron YM-30 filter units (Millipore), washed, and incubated with trypsin (V5111; Promega) overnight in a humidified chamber. The following day, the filters were eluted and spun, and eluted samples were mixed with formic acid (final 5%) and dried (speed-vac). Samples were analyzed on the TripleTOF 5600 System by data-dependent acquisition (Supplementary Table 1).

Statistical Analysis

Results are expressed as means ± SE. Statistical significance was assessed by one-way or two-way ANOVA using Bonferroni multiple comparison post-test or by unpaired Student t test using GraphPad Prism 5.02 (GraphPad Software, San Diego, CA). A P value <0.05 was considered to be statistically significant.

RESULTS

To identify mechanisms linking GLP-1R signaling to increases in pancreatic mass, we analyzed pancreata from WT normoglycemic mice treated with Ex-4 for 1 week. Ex-4 increased absolute pancreas weight and pancreas weight normalized to body weight without significantly affecting body weight (Fig. 1*A*, Supplementary Fig. 1*A–C*, and Supplementary Fig. 2*B* and *C*) or lung weight (Supplementary Fig. 1*C*). As some gastrointestinal actions of GLP-1R agonists exhibit tachyphylaxis with sustained activation of GLP-1R signaling (16), we treated mice with Ex-4 for 4 weeks. Pancreatic weight remained significantly increased after 4 weeks of Ex-4 administration, at levels comparable to those observed in Ex-4–treated mice after 1 week (Fig. 1*B* and *C*). The increase in pancreas weight was not due to increased water content (edema), as wet-dry pancreatic weights were comparable in control versus Ex-4–treated mice (Fig. 1*D*). Surprisingly, DNA content was lower, despite increased pancreatic mass, after Ex-4 administration (Fig. 1*D*). Furthermore, no significant differences in proliferating (Ki67^{+}) cells were detected at 4, 12, 24, or 96 h following administration of Ex-4 (Fig. 1*E*). Additionally, levels of mRNA transcripts for genes regulating cell cycle progression, including *c-myc*, *cyclin D1*, *cyclin D2*, or the cyclin-dependent kinase inhibitor *p21cip* (Supplementary Fig. 2*E* and *F*), were significantly lower (*c-myc*, *cyclin D2*, and *p21cip*) or unchanged (*cyclin D1*) following Ex-4 administration. In contrast, protein content and the protein-to-DNA ratio were significantly increased in the pancreas of Ex-4–treated mice (Fig. 1*D* and Supplementary Fig. 2*D*). An increase in pancreatic mass was also detected following administration of the GLP-1R agonist liraglutide (Fig. 1*F*). Although acinar cells in the murine exocrine pancreas do not express the *Glp1r* (6), stereological quantification revealed that the increase in pancreas mass following Ex-4

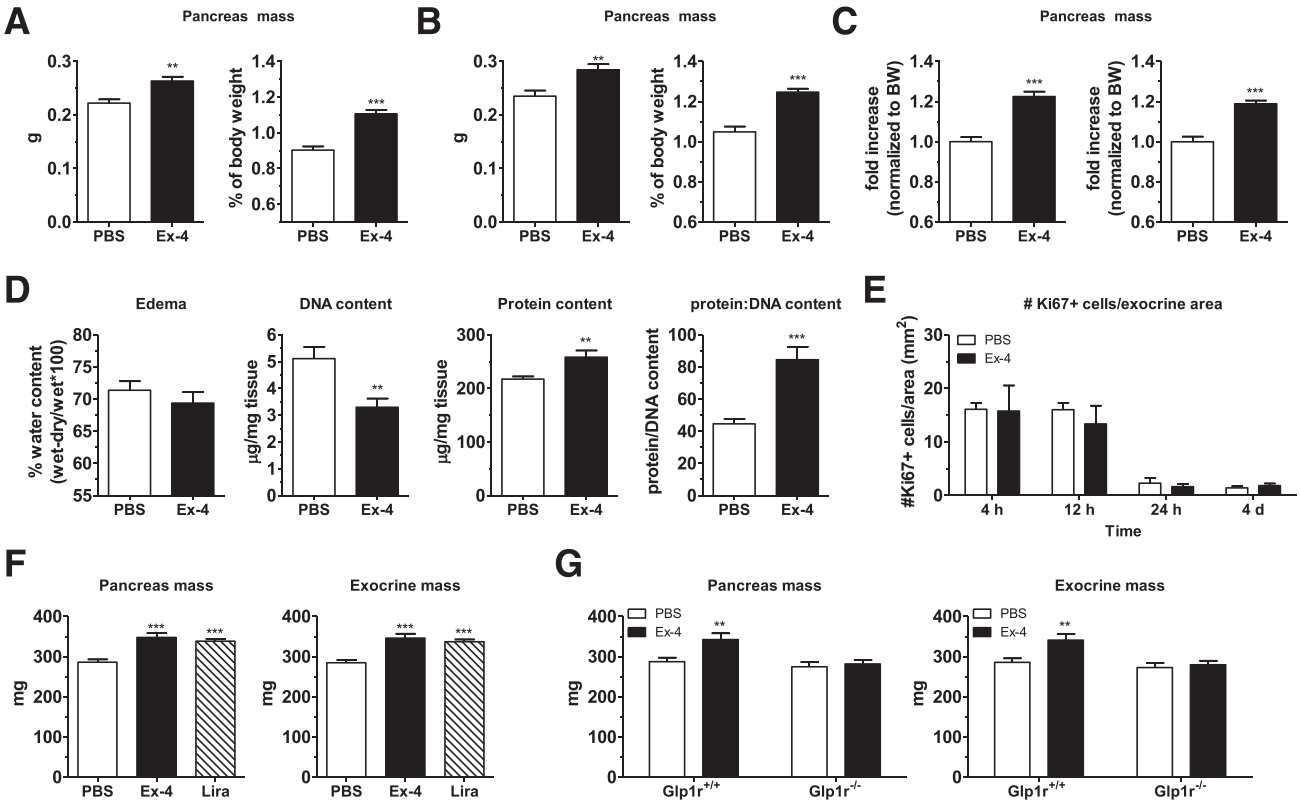

Figure 1—GLP-1R agonists increase pancreas weight. *A–C*: C57BL/6 mice were administered exogenous Ex-4 (10 nmol/kg, b.i.d.) or vehicle (PBS) for 7 days (*A*) or 4 weeks (*B*). Pancreas weight is shown as absolute weight (left panels) or as a percent of the final body weight (right panels). *C*: Pancreas weight in Ex-4–treated mice is shown as a fold increase relative to pancreas weight in PBS-treated mice treated after 7 days (left panel) or 4 weeks (right panel) of treatment. $n = 9$ (7 days) or $n = 10$ (4 weeks) in each group. Data are means ± SE. $^{**}P < 0.01$ and $^{***}P < 0.001$, Ex-4 vs. PBS. *D*: Water content (edema), DNA, and protein content in the pancreas of mice treated with Ex-4 or PBS for 4 weeks. Edema was calculated following desiccation and is expressed as a percentage of wet weight (wet weight − dry weight/wet weight × 100). DNA and protein content are expressed per milligram of pancreatic tissue. $n = 10$ in each group. Data are means ± SE. $^{**}P < 0.01$ and $^{***}P < 0.001$, Ex-4 vs. PBS. *E*: Quantification of Ki67$^+$ cells in the exocrine pancreas of C57BL/6 mice treated with Ex-4 or PBS for 4–96 h. Shown is the number of Ki67$^+$ cells per exocrine area analyzed. *F–G*: Stereological quantification of pancreatic exocrine mass of C57BL/6 mice administered exogenous Ex-4, liraglutide (Lira), or PBS for 14 days ($n = 10$ in each group) (*F*) or *Glp1r*$^{+/+}$ and *Glp1r*$^{-/-}$ littermate controls administered exogenous Ex-4 or PBS for 14 days ($n = 10$–12 in each group) (*G*). The total pancreas mass and total exocrine pancreas mass were quantified using manual point-counting using newCAST software (Visiopharm). Corrected pancreas mass excludes nonpancreatic tissue elements, e.g., lymph and fat. The exocrine mass was determined as the corrected pancreas mass with the endocrine mass excluded. The total mass of ductal epithelial cells was quantified by manual point-counting of ck19-labeled duct cells. Quantification of β-cell and non–β-cell masses was done by automatic image analysis of immunohistochemically labeled sections using Visiomorph software (Visiopharm). Shown is the corrected pancreas mass (pancreas mass excluding nonpancreatic tissue elements, e.g., lymph and fat) and exocrine mass (corrected pancreas mass–endocrine mass). Data are means ± SE. $^{**}P < 0.01$ and $^{***}P < 0.001$ vs. control.

or liraglutide was due to an increase in the mass of the exocrine pancreas (Fig. 1*F*). In contrast, no significant changes in relative proportions of endocrine, β-cell, ductal, or non–β-cell compartments were detected in mice treated with Ex-4 or liraglutide (Supplementary Fig. 1*D*). Consistent with the essential role for the canonical GLP-1R in transducing the metabolic and glucoregulatory actions of GLP-1R agonists in mice (12,17), Ex-4 had no effect on pancreatic or exocrine mass in *Glp1r*$^{-/-}$ mice (Fig. 1*G* and Supplementary Fig. 1*E*).

As recent studies have linked nutrient-stimulated CCK release to activation of GLP-1 secretion (18), and CCK potently increases pancreatic protein synthesis (19), we assessed whether the actions of GLP-1R agonists to increase pancreatic mass (and protein) required CCK receptors. Ex-4 administration augmented pancreas weight similarly in mice lacking either *Cckar*$^{-/-}$ or *Cckbr*$^{-/-}$ or in *Cckar*$^{-/-}$:*Cckbr*$^{-/-}$ mice lacking both CCK receptors (Fig. 2*A* and *B*). We next queried whether endogenous GLP-1R signaling was required for the adaptive increase in pancreatic mass in response to an HPD (20); however, pancreas weight was increased to a similar extent in HPD-fed *Glp1r*$^{+/+}$ versus *Glp1r*$^{-/-}$ mice (Fig. 2*C*).

Analysis of key proteins controlling the initiation of protein synthesis (Fig. 3*A–C*) revealed that Ex-4 initially reduced the phosphorylation of the 40*S* ribosomal subunit S6; however, a significant increase in S6 phosphorylation was detected by 12 h after Ex-4 treatment (Fig. 3*A* and *C*), with further robust increases evident in pancreata from mice treated with Ex-4 from 2–7 days (Fig. 3*B* and

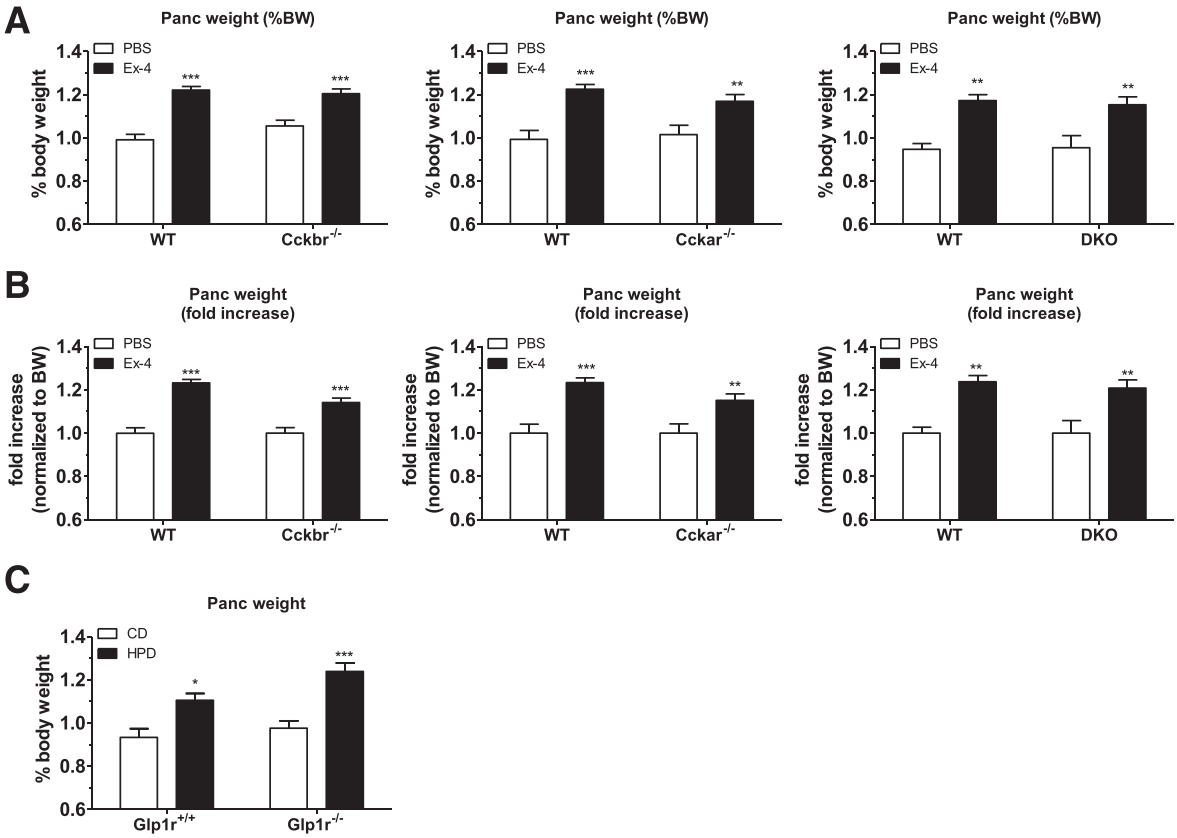

Figure 2—*A* and *B*: *Cckbr*$^{-/-}$, *Cckar*$^{-/-}$, *Cckar*$^{-/-}$:*Cckbr*$^{-/-}$ (DKO), and WT littermate control mice were administered exogenous Ex-4 or vehicle (PBS) for 10 days. Pancreas weight is shown as a percent of the final body weight (BW) (*A*) or as a fold increase relative to PBS-treated mice (normalized to BW) (*B*). Results are expressed as means ± SE. $^{**}P < 0.01$ and $^{***}P < 0.001$, Ex-4 vs. PBS. n = 6–10 female mice in each group. *C*: Pancreas weight shown as a percent of final body weight in *Glp1r*$^{+/+}$ and *Glp1r*$^{-/-}$ mice maintained on CD or HPD for 7 days. Results are expressed as means ± SE. $^{*}P < 0.05$ and $^{***}P < 0.001$, HPD vs. CD. n = 4–6 in each group. Panc, pancreas.

C). Similar results were seen for the γ isoform of the translational repressor 4EBP1 (Fig. 3*A*–*C*). The induction of S6 phosphorylation required the canonical GLP-1R, as S6 phosphorylation was not observed in the pancreas of Ex-4–treated *Glp1r*$^{-/-}$ mice (Fig. 3*D*). Moreover, cytoplasmic staining of phosphorylated S6 was observed in acinar cells (Supplementary Fig. 5*B*).

As the mTOR pathway plays a pivotal role in the regulation of protein synthesis (21), we examined the requirement for this pathway in the GLP-1R–mediated increase in pancreas weight. Treatment with the mTOR complex 1 (mTORC1) inhibitor rapamycin had no significant effect on body weight (Supplementary Fig. 3*A*) but completely abolished the Ex-4–induced increase in pancreas weight (Fig. 3*E*) and S6 phosphorylation (Fig. 3*G*). However, the actions of Ex-4 to increase small bowel mass (22) were not diminished in rapamycin-treated mice (Fig. 3*F*). Moreover, rapamycin did not attenuate the Ex-4 induction of *Slc3a1*, *Reg3β*, or *Reg3α* nor the suppression of *p21cip* in the pancreas from the same experiments (Fig. 3*H*).

We next assessed whether activation of GLP-1R signaling regulated expression of genes encoding pancreatic enzymes, as plasma levels of amylase and lipase are modestly increased in some human subjects treated with GLP-1R agonists (3). Lipase mRNA levels were lower in the pancreas of Ex-4–treated mice, whereas levels of amylase were not significantly different (Fig. 4*A* and *C*). Consistent with these findings, serum lipase levels were reduced and amylase levels were unchanged in Ex-4–treated mice; however, both lipase and amylase levels were markedly induced after caerulein administration (Fig. 4*D*). Ex-4 also rapidly increased levels of pancreatic mRNA transcripts for the anti-inflammatory genes *socs3* and *Reg3β* (Fig. 4*B*). *Socs3* mRNA transcripts returned to normal by 24 h despite ongoing Ex-4 administration; however, *Reg3β* mRNA transcripts remained elevated in the pancreas of mice treated with Ex-4 (Fig. 4*B* and *C*). Furthermore, the induction of both *Reg3α* and *Reg3β* by Ex-4 or liraglutide requires the GLP-1R, as neither of these transcripts were upregulated in the pancreas of *Glp1r*$^{-/-}$ mice treated with GLP-1R agonists (8,14). Ex-4 reduced levels of lipase and increased *Reg3* mRNA transcripts in pancreata of rapamycin-treated mice (Fig. 4*E* and Fig. 3*H*), indicating divergent mechanisms for GLP-1R–dependent control of pancreatic protein synthesis versus gene expression. In contrast, Ex-4 did not alter levels of mRNA transcripts encoding the cationic amino acid transporter *slc7a1*, the glucose transporter *glut2*, pyruvate dehydrogenase

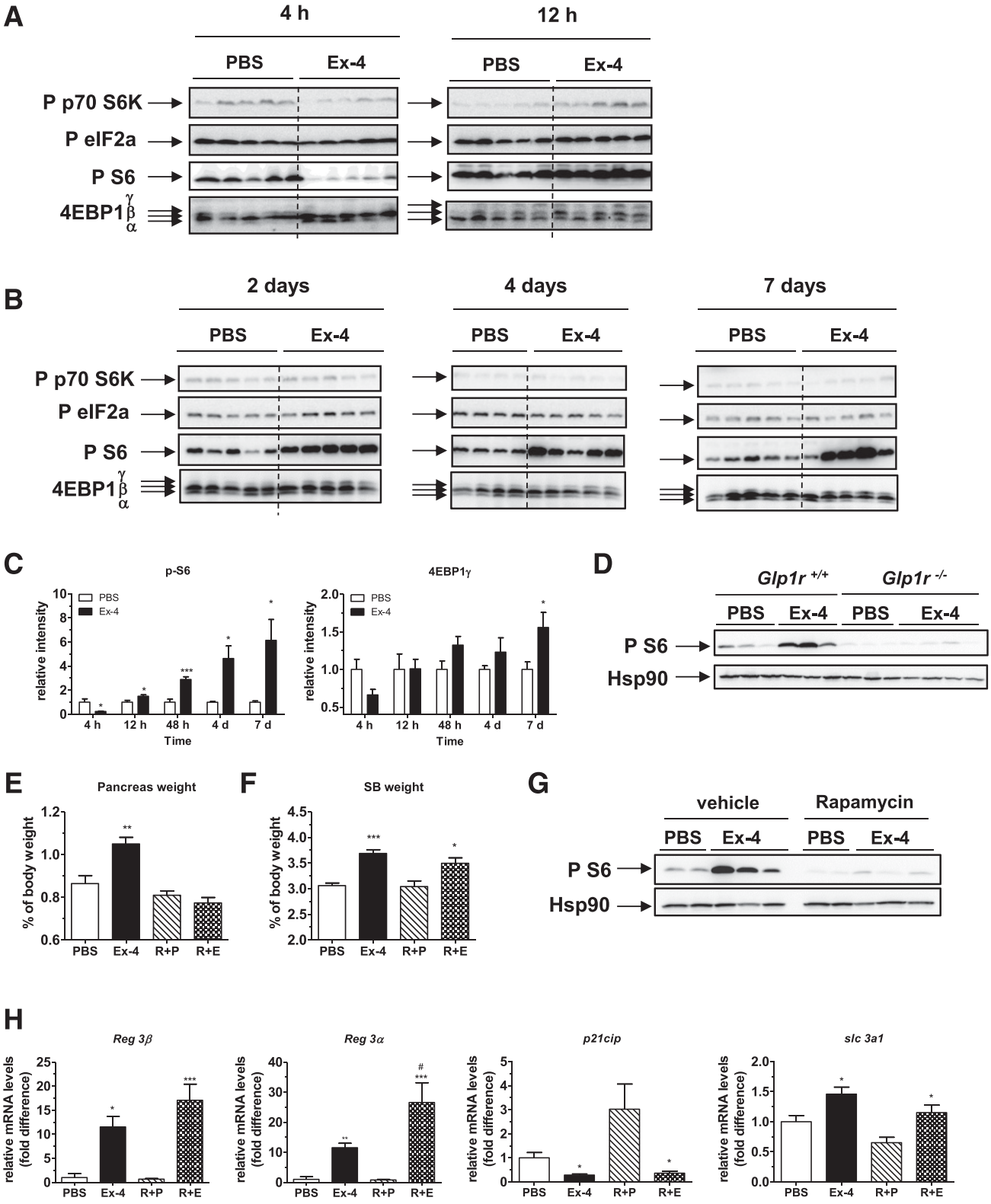

Figure 3—Western blot analysis of whole-cell lysates of pancreas tissue from C57BL/6 mice administered exogenous Ex-4 or vehicle (PBS) for 4 or 12 h (*A*) or 2–7 days (*B*) as indicated. Each lane represents pancreatic protein from an individual mouse. *C*: Quantification of levels of phosphorylated S6 and the abundance of the hyperphosphorylated form of 4EBP1 (4EBP1γ form of 4EBP1) from panels *A* and *B*. **P* < 0.05 and ****P* < 0.001, Ex-4 vs. PBS. *D*: Western blot analysis of whole-cell pancreas lysates from *Glp1r*$^{+/+}$ and *Glp1r*$^{-/-}$ mice administered Ex-4 or PBS for 3 days. Each lane represents an individual mouse. Pancreas weight (*E*) and small bowel weight (*F*) as a percentage of body weight of male C57BL/6 mice administered vehicle or rapamycin (2 mg/kg 1× daily, i.p.) together with Ex-4 or PBS for 7 days. **P* < 0.05, ***P* < 0.01, and ****P* < 0.001 vs. control. *G*: Western blot analysis of pancreatic lysates from WT mice administered vehicle or rapamycin 30 min prior to Ex-4 or PBS for 3 days. Each lane represents an individual mouse. *H*: Quantitative PCR analysis of RNA isolated from the

kinase isozyme 4 (*pdk4*), the exocrine transcription factor *mist1*, or *Cckar* and *Cckbr* in the murine pancreas (Supplementary Fig. 3*B*).

To further characterize changes in the pancreatic proteome following activation of GLP-1R signaling, we performed a proteomics analysis on whole pancreas tissue after 1 week of Ex-4 administration. Spectral counting analysis was performed to identify proteins that were specifically regulated by Ex-4. The majority of proteins in the pancreas were proportionately increased to a similar extent by Ex-4 treatment (Supplementary Table 1); however, some proteins were preferentially increased or underrepresented following Ex-4 administration. A summary of the most striking differences in relative protein abundance following Ex-4 treatment is shown in Table 1, including Reg3β and Reg2, which were not detected in the pancreas of vehicle-treated mice (Table 1 and Supplementary Table 1). Similarly, fatty acid binding protein 5 (Fabp5) and P450 cytochrome oxidoreductase (Por), proteins involved in fatty acid uptake and lipid oxidation, were detected at low levels in the pancreas of vehicle-treated mice but were abundant following Ex-4 treatment. Other proteins upregulated by Ex-4 (Table 1 and Supplementary Table 1) include those involved in protein translation and secretion, including family with sequence similarity 129 member A (Fam129a), eIF4a1, tryptophanyl-tRNA synthetase (Wars), and deleted in malignant brain tumors 1 (Dmbt1). Notably, we did not detect preferential upregulation of amylase or lipase proteins after Ex-4 administration (Supplementary Table 2).

An increase in protein abundance can reflect changes in both transcription and translation; hence, we examined levels of mRNA transcripts for proteins preferentially increased by Ex-4. Ex-4 induced expression of the *Reg* genes (*Reg3*, *Reg2*, and *Reg1*) and modestly upregulated *dmbt1* transcripts after 1 week of treatment (Fig. 3*H*, Fig. 4*B*, and Supplementary Fig. 4*A*), whereas *Reg1* and *dmbt1* transcript levels were not different after 1 month of Ex-4 administration (Supplementary Fig. 4*B*). Ex-4 did not affect levels of mRNA transcripts for many of the other Ex-4–induced proteins, including *por*, *fabp5*, *fam129a*, *wars*, or *eif4a1* (Supplementary Fig. 4*A* and *B*), suggesting that the Ex-4–induced increase of these particular proteins was regulated at the translational level. The relative mRNA levels of *reg2, reg3β, reg1*, and *dmbt1*, as well as *lipase*, *amylase*, and *colipase*, were 100–1,000 times less abundant in RNA isolated from islets when compared with whole pancreas (Supplementary Fig. 4*C*), suggesting that these genes are predominantly expressed in the exocrine pancreas. These findings are consistent with predominant localization of Reg3 protein expression to the exocrine pancreas (Supplementary Fig. 5*A*). In contrast, the differences in relative mRNA levels for *por*, *fabp5*, *wars*, and *eif4a1* were not as robust in whole pancreas versus islets, suggesting that these genes are expressed in both endocrine and exocrine compartments (Supplementary Fig. 4*C*). As expected, the *Gcg*, *Glp1r*, and *Ins*2 genes were preferentially expressed in islet RNA (Supplementary Fig. 4*C*).

DISCUSSION

Although it is often assumed that GLP-1R agonists increase pancreas weight through stimulation of exocrine cell proliferation, evidence in support of this hypothesis has not been forthcoming (3,4). Our findings that Ex-4 or liraglutide have no effect on total endocrine cell mass, β-cell mass, or the mass of ductal epithelium in normoglycemic mice are consistent with an important role for hyperglycemia in the GLP-1R–dependent stimulation of pancreatic islet cell proliferation (7,14,23,24). Indeed, some studies have reported that GLP-1R agonists reduce β-cell mass in normoglycemic animals (25), possibly reflecting weight loss and increased insulin sensitivity. One study described increased acinar cell proliferation in chow-fed mice treated with liraglutide; however, acinar cell proliferation was not increased in high fat–fed mice treated with liraglutide (25). In contrast, there were no significant effects of GLP-1R agonists on growth and proliferation of human pancreatic adenocarcinoma cell lines (26,27). Hence, there is little evidence linking activation of GLP-1R signaling to the proliferation of normal or neoplastic pancreatic acinar cells.

Levels of mRNA transcripts for the cyclin-dependent kinase inhibitor *p21cip* declined following Ex-4 administration; however, a reduction in mRNA levels was also observed for genes promoting cell cycle progression, including *c-myc* and *cyclin D2*, whereas *cyclin D1* remained unchanged. Importantly, rapamycin abolished the Ex-4–induced increase in pancreas weight but did not attenuate the suppression of *p21cip* by Ex-4, demonstrating that downregulation of *p21cip* transcript levels occurs independently of changes in pancreas mass. Furthermore, the number of $Ki67^+$ cells in the exocrine compartment and total DNA content in the pancreas were not induced by Ex-4; indeed, DNA content was lower after 4 weeks of Ex-4 administration, despite increased pancreatic mass. Taken together, it seems unlikely that GLP-1R signaling promotes exocrine cell proliferation within the context of the experimental paradigm presented herein.

GLP-1R agonists increase pancreatic mass and protein synthesis through mechanisms requiring the known GLP-1 receptor, but it remains unclear how the GLP-1R–dependent signal is relayed to pancreatic acinar cells. GLP-1R–dependent stimulation of insulin secretion is a logical candidate for

pancreas of the above treated mice. The levels of the indicated transcripts were determined by real-time PCR, normalized to cyclophilin (*Ppia*) mRNA content. Results are expressed as means ± SE. $^*P < 0.05$, $^{**}P < 0.01$, and $^{***}P < 0.001$, Ex-4 vs. PBS; $\#P < 0.05$, rapamycin vs. vehicle. $n = 5$ in each group. E, Ex-4; P, PBS; R, rapamycin; SB, small bowel.

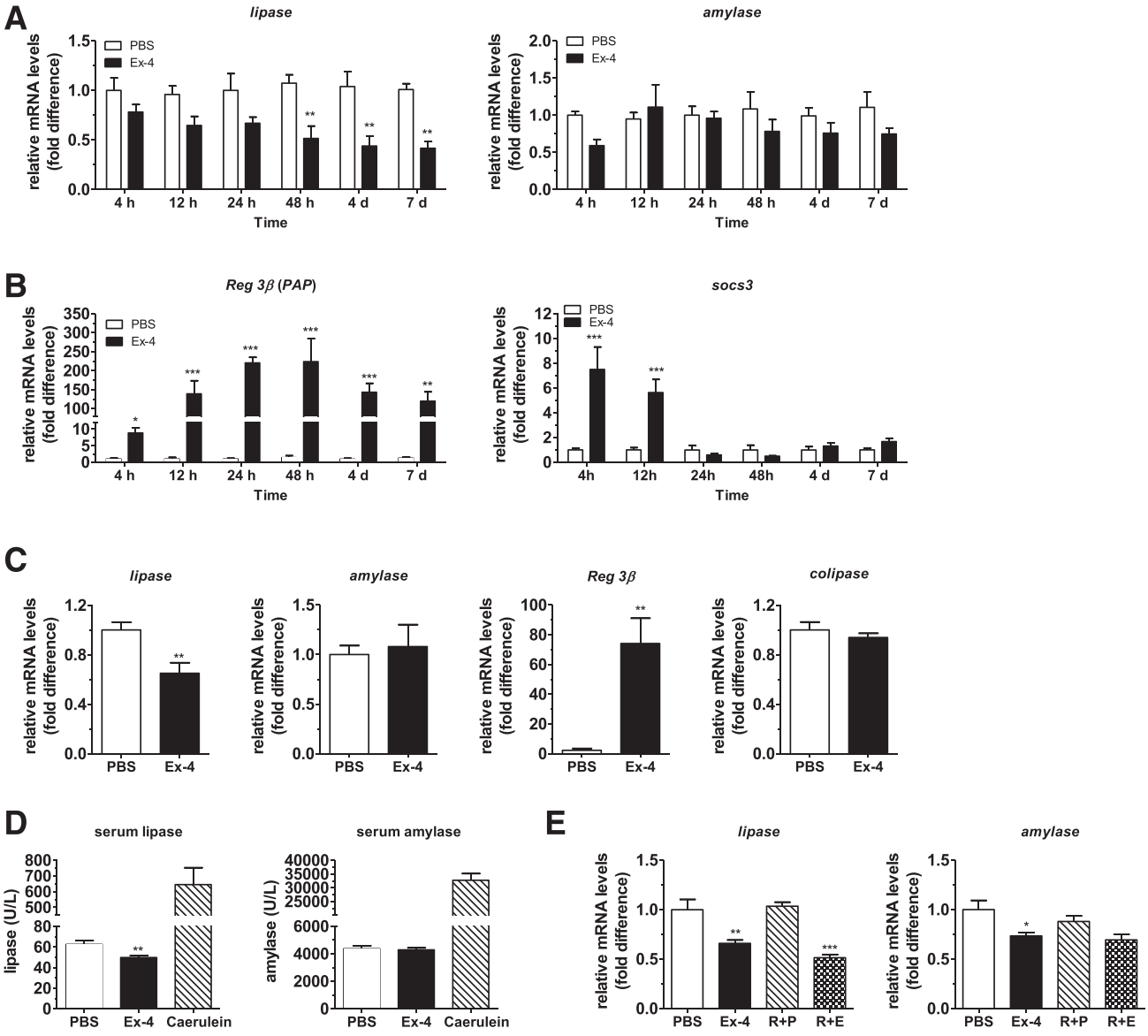

Figure 4— Quantitative PCR analysis of RNA isolated from the pancreas of mice treated with Ex-4 or PBS for 4 h to 7 days (*A* and *B*), Ex-4 or PBS for 4 weeks (*C*), or Ex-4 or PBS for 7 days with or without coadministration of rapamycin (*E*). The levels of the indicated transcripts were determined by real-time PCR, normalized to cyclophilin (*Ppia*) mRNA content. Results are expressed as a fold difference relative to PBS and expressed as means ± SE. **P* < 0.05, ***P* < 0.01, and ****P* < 0.001, Ex-4 vs. PBS. *n* = 5 male C57BL/6 mice (*A* and *B*), *n* = 12 male and female mice (*C*), or *n* = 5 male C57BL/6 mice in each group (*E*). *D*: Enzymatic lipase and amylase levels in serum from C57BL/6 mice administered Ex-4 or PBS for 1 month (*n* = 10 in each group) or administered five sequential hourly intraperitoneal injections of caerulein, 50 μg/kg body weight (*n* = 2) as described in RESEARCH DESIGN AND METHODS. Results are expressed as means ± SE. ***P* < 0.01, Ex-4 vs. PBS. U, units.

islet-acinar communication (28); hence, we studied normoglycemic mice to minimize confounding effects of increased insulin secretion. Evidence against a role for insulin as an indirect GLP-1R–dependent stimulator of pancreatic protein synthesis and mass derives from studies using genetic selective restoration of hGLP1R expression in murine β-cells of *Glp1r*$^{-/-}$ mice (14). Although GLP-1R agonists robustly increased insulin secretion and lowered glycemia in hGLP1R:*Glp1r*$^{-/-}$ mice, Ex-4 had no effect on pancreatic mass or pancreatic expression of Reg3α or Reg3β in hGLP1R:*Glp1r*$^{-/-}$ mice (14), indicating that increased levels of insulin are not sufficient to mediate the effects of GLP-1R agonists on the exocrine pancreas.

CCK activates GLP-1–containing neurons in the central nervous system (29,30), and GLP-1 and CCK are colocalized in and secreted from subsets of enteroendocrine L cells (31). Pancreatic growth is readily induced by CCK administration or administration of exogenous protease/trypsin inhibitors that elevate levels of CCK (32). Nevertheless, CCK agonists and protease inhibitors simultaneously induce cell proliferation and protein synthesis, whereas GLP-1R agonists increased pancreatic mass without

Table 1—Summary of proteomic analysis in whole pancreas tissue of male C57BL/6 mice administered Ex-4 or vehicle for 7 days

Gene ID	Gene name	Protein name	Function	Fold change
19693	Reg2	Pancreatic thread/stone protein 2	Expressed in regenerating islets and normal exocrine pancreas Stimulates growth of β-cells	1,224.62
18489	Reg3β	Regenerating islet-derived 3 β	Anti-inflammatory Secreted protein that contains a C-type lectin domain involved in carbohydrate binding	325.09
18984	Por	P450 (cytochrome) oxidoreductase	Required for electron transport from NADP to cytochrome P450 in the ER and mitochondrial membrane (e.g., lipid oxidation)	155.60
16592	Fabp5	Fatty acid binding protein 5	Plays a role in fatty acid uptake, transport, and metabolism	51.05
63913	Fam129a	Family with sequence similarity 129 member A	Regulates phosphorylation of proteins involved in translation (eIF2a, EIF4EBP1,RPS6KB1) May be involved in ER stress response	49.20
74915	Atp6v1e2	V1-type proton ATPase subunit E 2	Enzyme transporter that functions to acidify intracellular compartments in eukaryotic cells Important role in receptor-mediated endocytosis, protein degradation, and coupled transport	12.65
436523	Gm5771	Trypsinogen 12	Trypsin 12 precursor (zymogen)	11.27
22073	Prss3	Trypsinogen 3	Mesotrypsin precursor (zymogen)	10.67
103964	Try5	Trypsin 5	Trypsin-like serine protease	8.77
11720	Mat1a	Methionine adenosyl-transferase I, α	Catalyzes the transfer of the adenosyl moiety of ATP to methionine to form S-adenosyl-methionine (source of methyl groups for most biological methylations)	6.55
17880	Myh11	Smooth muscle myosin heavy chain 11	Functions as a major contractile protein	6.25
436522	Try10	Trypsinogen 10	Trypsin 10 precursor (zymogen)	4.42
19692	Reg1	Regenerating islet-derived 1/pancreatic stone protein 1 (PSP1)	Associated with islet cell regeneration Stimulates growth of β-cells Might act as an inhibitor of spontaneous calcium carbonate precipitation	3.95
13681	eIF4a1	Eukaryotic translation initiation factor 4A1	Subunit of the eIF4F complex involved in cap recognition and is required for mRNA binding to ribosomes	2.90
12945	Dmbt1	Deleted in malignant brain tumors 1	Involved in remodeling during exocytosis Interacts with pancreatic zymogens Involved in secretion of acinar cells	2.84
66473	Ctrb1	Chymotrypsinogen B1	Inactive serine protease precursor (zymogen)	2.32
22375	Wars	Tryptophanyl-tRNA synthetase	"Attach" tryptophan to its tRNA Induced by interferon	2.32
16612	Klk1	Glandular kallikrein 1	Cleave Met-Lys and Arg-Ser bonds in kininogen to release the vasoactive peptide, Lys-bradykinin from kininogen	2.31
319188	Hist1h2bp	Histone cluster 1, H2bp	A member of the histone H2B family	2.24
230721	Pabpc4	Poly(A) binding protein, cytoplasmic 4 inducible poly(A) binding protein	May be necessary for regulation of stability of labile mRNA species in activated T cells Isolated as an activation-induced T-cell mRNA encoding protein	−2.39
14118	Fbn1	Fibrillin 1	Structural components of 10–12-nm extracellular calcium-binding microfibrils	−4.45
209027	Pycr1	Pyrroline-5-carboxylate reductase 1	Enzyme that catalyzes the last step in proline biosynthesis	−17.5
22074	Try4	Trypsin 4	Trypsin 4 precursor	−1,023.29

Shown are proteins with fold changes >2 and false discovery rates ≤0.05 from spectral count analysis of whole pancreas following Ex-4 administration. False discovery rate is the error rate estimated for a particular *z* statistic threshold calculated from the replicate data consistency and degree of change between control (PBS) and experimental (Ex-4) sample. Scale of 0–1, with 1 being random. *Z* statistic (log fold change divided by the standard error of log fold change) measures the statistical significance of the change.

concomitant changes in cell proliferation or DNA content. Although the overlapping actions of CCK and GLP-1R agonists raised the possibility that GLP-1R agonists increase pancreas mass through direct or indirect activation of CCK receptor signaling, the trophic effects of GLP-1R agonists were preserved in mice with inactivation of one or both CCK receptors. Hence, CCK signaling is not required for the effects of GLP-1R agonists to increase pancreatic mass.

The results of our proteomic analyses demonstrate that Ex-4 differentially induces the expression of proteins involved in aspects of nutrient uptake, protein translation, protein folding, or exocytosis. An unresolved question is whether the small increase in serum levels of lipase, and to a lesser extent, amylase, observed in some patients treated with GLP-1R agonists (3) reflects the actions of these agents to increase pancreatic protein synthesis. We did not observe increases in pancreatic amylase gene expression, and lipase mRNA transcripts were significantly lower after Ex-4 administration. Furthermore, studies of pancreatic enzyme levels in rodents have been inconsistent, demonstrating either no change or small increases in amylase following administration of GLP-1R agonists (17,33–35). Our current studies demonstrate that serum lipase levels were lower, whereas amylase levels and pancreatic content of amylase and lipase proteins (Supplementary Table 2) remained similar after treatment with Ex-4. Hence, nondiabetic mice do not reveal a putative mechanism linking GLP-1R signaling to the expression or activity of amylase and lipase.

Although Ex-4 treatment proportionately increased the majority of proteins in the pancreas to a similar extent, some proteins, including Reg3, Reg2, and Reg1, were preferentially increased by Ex-4. The Reg proteins are small secreted proteins belonging to the calcium-dependent lectin (C-type lectin) superfamily, encoded by four genes (*Reg1*, *-2*, *-3*, and *-4*). Reg1 is predominantly localized to acinar cells; however, it may be upregulated in islets under pathological conditions, including pancreatic resection or diabetes (36). Although it is unclear how Ex-4 induces *Reg* gene and protein expression, *Reg* expression is induced by proinflammatory cytokines, growth factors, and experimental pancreatic injury (36). Some investigators have inferred that induction of pancreatic Reg3 expression reflects the presence of mild subclinical pancreatitis (37); however, Reg proteins, including Reg3, also exert anti-inflammatory actions (38), and reduction of Reg expression significantly worsened the severity of experimental pancreatitis in rats (39). Furthermore, our unbiased analysis of the entire pancreatic proteome did not reveal a protein profile suggestive of a proinflammatory state following Ex-4 administration (Supplementary Table 1). Hence, the biological significance of the robust GLP-1R–dependent induction of *Reg* gene and protein expression in the exocrine pancreas requires further investigation.

In summary, activation of the GLP-1R rapidly increases pancreatic gene and protein expression and pancreatic weight in mice. The cellular site(s) of GLP-1R expression important for transduction of these signals to the exocrine pancreas remains unclear; however, the available evidence suggests that these effects are indirect and not mediated through acinar *Glp1r* expression (6). Our data open a new area of research into understanding how GLP-1R signaling communicates with the exocrine pancreas and explain previous observations of increased pancreas weight following pharmacological administration of GLP-1R agonists in preclinical studies.

Funding. D.J.D. was supported in part by the Canada Research Chairs Program and a Banting & Best Diabetes Centre–Novo Nordisk Chair in Incretin Biology. J.E.C. was supported by a Canadian Institutes of Health Research postdoctoral fellowship. These studies were funded in part by operating grant support from *1*) the Canadian Institutes of Health Research (123391) and *2*) Novo Nordisk.

Duality of Interest. T.S. and J.J. are employees of Gubra. D.J.D. has been a consultant to Novo Nordisk and other companies that develop and/or sell incretin-based therapies, including Arisaph Pharmaceuticals, Intarcia Therapeutics, Inc., Merck Research Laboratories, MedImmune, Receptos, Inc., Sanofi, Takeda, and Transition Therapeutics, Inc. Neither D.J.D. nor his family members hold stock directly or indirectly in any of these companies. No other potential conflicts of interest relevant to this article were reported.

Author Contributions. J.A.K., L.L.B., X.C., T.A., J.E.C., T.S., J.J., and B.L. performed experiments, analyzed data, and wrote and reviewed the manuscript. D.J.D. designed experiments, reviewed data, and wrote the manuscript. D.J.D. is the guarantor of this work and, as such, had full access to all the data in the study and takes responsibility for the integrity of the data and the accuracy of the data analysis.

References

1. Campbell JE, Drucker DJ. Pharmacology, physiology, and mechanisms of incretin hormone action. Cell Metab 2013;17:819–837

2. Drucker DJ, Nauck MA. The incretin system: glucagon-like peptide-1 receptor agonists and dipeptidyl peptidase-4 inhibitors in type 2 diabetes. Lancet 2006;368:1696–1705

3. Egan AG, Blind E, Dunder K, et al. Pancreatic safety of incretin-based drugs—FDA and EMA assessment. N Engl J Med 2014;370:794–797

4. Drucker DJ. Incretin action in the pancreas: potential promise, possible perils, and pathological pitfalls. Diabetes 2013;62:3316–3323

5. Nauck MA. A critical analysis of the clinical use of incretin-based therapies: the benefits by far outweigh the potential risks. Diabetes Care 2013;36:2126–2132

6. Richards P, Parker HE, Adriaenssens AE, et al. Identification and characterization of GLP-1 receptor-expressing cells using a new transgenic mouse model. Diabetes 2014;63:1224–1233

7. Baggio LL, Huang Q, Cao X, Drucker DJ. An albumin-exendin-4 conjugate engages central and peripheral circuits regulating murine energy and glucose homeostasis. Gastroenterology 2008;134:1137–1147

8. Koehler JA, Baggio LL, Lamont BJ, Ali S, Drucker DJ. Glucagon-like peptide-1 receptor activation modulates pancreatitis-associated gene expression but does not modify the susceptibility to experimental pancreatitis in mice. Diabetes 2009;58:2148–2161

9. Gotfredsen CF, Mølck AM, Thorup I, et al. The human GLP-1 analogs liraglutide and semaglutide: absence of histopathological effects on the pancreas in nonhuman primates. Diabetes 2014;63:2486–2497

10. Parkes DG, Mace KF, Trautmann ME. Discovery and development of exenatide: the first antidiabetic agent to leverage the multiple benefits of the incretin hormone, GLP-1. Expert Opin Drug Discov 2013;8:219–244

11. Hansotia T, Baggio LL, Delmeire D, et al. Double incretin receptor knockout (DIRKO) mice reveal an essential role for the enteroinsular axis in transducing the glucoregulatory actions of DPP-IV inhibitors. Diabetes 2004;53:1326–1335

12. Scrocchi LA, Brown TJ, MaClusky N, et al. Glucose intolerance but normal satiety in mice with a null mutation in the glucagon-like peptide 1 receptor gene. Nat Med 1996;2:1254–1258
13. Dalbøge LS, Almholt DL, Neerup TS, et al. Characterisation of age-dependent beta cell dynamics in the male db/db mice. PLoS ONE 2013;8:e82813
14. Lamont BJ, Li Y, Kwan E, Brown TJ, Gaisano H, Drucker DJ. Pancreatic GLP-1 receptor activation is sufficient for incretin control of glucose metabolism in mice. J Clin Invest 2012;122:388–402
15. Wiśniewski JR, Zougman A, Nagaraj N, Mann M. Universal sample preparation method for proteome analysis. Nat Methods 2009;6:359–362
16. Drucker DJ, Buse JB, Taylor K, et al.; DURATION-1 Study Group. Exenatide once weekly versus twice daily for the treatment of type 2 diabetes: a randomised, open-label, non-inferiority study. Lancet 2008;372:1240–1250
17. Tatarkiewicz K, Sablan EJ, Polizzi CJ, Villescaz C, Parkes DG. Long-term metabolic benefits of exenatide in mice are mediated solely via the known glucagon-like peptide 1 receptor. Am J Physiol Regul Integr Comp Physiol 2014;306:R490–R498
18. Beglinger S, Drewe J, Schirra J, Göke B, D'Amato M, Beglinger C. Role of fat hydrolysis in regulating glucagon-like peptide-1 secretion. J Clin Endocrinol Metab 2010;95:879–886
19. Bragado MJ, Tashiro M, Williams JA. Regulation of the initiation of pancreatic digestive enzyme protein synthesis by cholecystokinin in rat pancreas in vivo. Gastroenterology 2000;119:1731–1739
20. Crozier SJ, Sans MD, Wang JY, Lentz SI, Ernst SA, Williams JA. CCK-independent mTORC1 activation during dietary protein-induced exocrine pancreas growth. Am J Physiol Gastrointest Liver Physiol 2010;299:G1154–G1163
21. Laplante M, Sabatini DM. mTOR signaling in growth control and disease. Cell 2012;149:274–293
22. Simonsen L, Pilgaard S, Orskov C, et al. Exendin-4, but not dipeptidyl peptidase IV inhibition, increases small intestinal mass in GK rats. Am J Physiol Gastrointest Liver Physiol 2007;293:G288–G295
23. Sturis J, Gotfredsen CF, Rømer J, et al. GLP-1 derivative liraglutide in rats with beta-cell deficiencies: influence of metabolic state on beta-cell mass dynamics. Br J Pharmacol 2003;140:123–132
24. Lamont BJ, Drucker DJ. Differential antidiabetic efficacy of incretin agonists versus DPP-4 inhibition in high fat fed mice. Diabetes 2008;57:190–198
25. Ellenbroek JH, Töns HA, Westerouen van Meeteren MJ, et al. Glucagon-like peptide-1 receptor agonist treatment reduces beta cell mass in normoglycaemic mice. Diabetologia 2013;56:1980–1986
26. Koehler JA, Drucker DJ. Activation of glucagon-like peptide-1 receptor signaling does not modify the growth or apoptosis of human pancreatic cancer cells. Diabetes 2006;55:1369–1379
27. Zhao H, Wei R, Wang L, et al. Activation of glucagon-like peptide-1 receptor inhibits growth and promotes apoptosis of human pancreatic cancer cells in a cAMP-dependent manner. Am J Physiol Endocrinol Metab 2014;306:E1431–E1441
28. Barreto SG, Carati CJ, Toouli J, Saccone GT. The islet-acinar axis of the pancreas: more than just insulin. Am J Physiol Gastrointest Liver Physiol 2010;299:G10–G22
29. Rinaman L. Interoceptive stress activates glucagon-like peptide-1 neurons that project to the hypothalamus. Am J Physiol 1999;277:R582–R590
30. Hisadome K, Reimann F, Gribble FM, Trapp S. CCK stimulation of GLP-1 neurons involves α1-adrenoceptor-mediated increase in glutamatergic synaptic inputs. Diabetes 2011;60:2701–2709
31. Habib AM, Richards P, Cairns LS, et al. Overlap of endocrine hormone expression in the mouse intestine revealed by transcriptional profiling and flow cytometry. Endocrinology 2012;153:3054–3065
32. Williams JA. Regulation of acinar cell function in the pancreas. Curr Opin Gastroenterol 2010;26:478–483
33. Tatarkiewicz K, Smith PA, Sablan EJ, et al. Exenatide does not evoke pancreatitis and attenuates chemically induced pancreatitis in normal and diabetic rodents. Am J Physiol Endocrinol Metab 2010;299:E1076–E1086
34. Vrang N, Jelsing J, Simonsen L, et al. The effects of 13 wk of liraglutide treatment on endocrine and exocrine pancreas in male and female ZDF rats: a quantitative and qualitative analysis revealing no evidence of drug-induced pancreatitis. Am J Physiol Endocrinol Metab 2012;303:E253–E264
35. Tatarkiewicz K, Belanger P, Gu G, Parkes D, Roy D. No evidence of drug-induced pancreatitis in rats treated with exenatide for 13 weeks. Diabetes Obes Metab 2013;15:417–426
36. Parikh A, Stephan AF, Tzanakakis ES. Regenerating proteins and their expression, regulation and signaling. Biomol Concepts 2012;3:57–70
37. Mondragon A, Davidsson D, Kyriakoudi S, et al. Divergent effects of liraglutide, exendin-4, and sitagliptin on beta-cell mass and indicators of pancreatitis in a mouse model of hyperglycaemia. PLoS ONE 2014;9:e104873
38. Loonen LM, Stolte EH, Jaklofsky MT, et al. REG3γ-deficient mice have altered mucus distribution and increased mucosal inflammatory responses to the microbiota and enteric pathogens in the ileum. Mucosal Immunol 2014;7:939–947
39. Zhang H, Kandil E, Lin YY, Levi G, Zenilman ME. Targeted inhibition of gene expression of pancreatitis-associated proteins exacerbates the severity of acute pancreatitis in rats. Scand J Gastroenterol 2004;39:870–881

SUPPLEMENTARY DATA

Supplementary Figure 1. A-B) Final body weights of C57BL/6 mice administered exogenous Ex-4 (10 nmol/kg, BID) or vehicle (PBS) for 7 days (A) or 4 weeks (B). n=9 (7 days) or n=10 (4 weeks) in each group. Data are means ± SE. C) Pancreas and lung weights (as a percentage of body weight) and final body weights of C57BL/6 mice treated with Ex-4 for 7 days. *n*=4 in each group. Data are means ± SE. ** p<0.01 Ex-4 *vs* PBS. D-E**)** Stereological quantification of pancreatic mass of D) C57BL/6 mice administered exogenous Ex-4, liraglutide, or vehicle (PBS) for 14 days. n=10 in each group, or E) *Glp1r*+/+ and *Glp1r*-/- littermate controls administered exogenous Ex-4, or vehicle (PBS) for 14 days. n=10-12 in each group. Shown is the endocrine mass (mass of beta and non-beta cells inside the islets), beta cell mass (insulin immunoreactivity), ductal epithelial mass (cytokeratin 19 immunoreactivity), and non-beta cell mass (glucagon, somatostatin and pancreatic polypeptide immunoreactivity). Data are means ± SE.

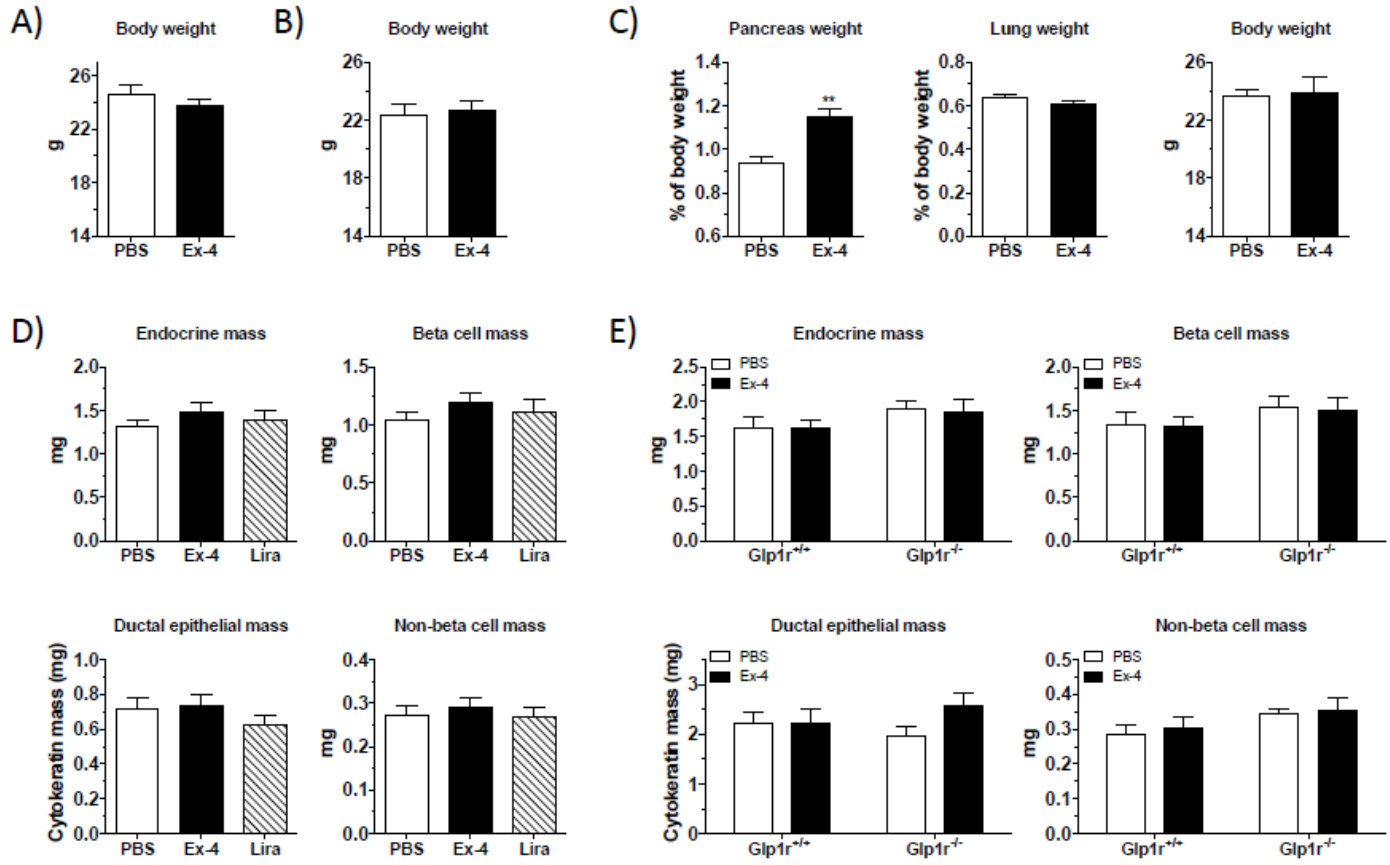

SUPPLEMENTARY DATA

Supplementary Figure 2. Ex-4 increases pancreas weight and protein content, but not DNA content following 7 days of treatment. Schematic representation of the experiment is shown in (A) and body weight in (B). C) Absolute pancreas weight (*left panel*) or pancreas weight (as a percentage of body weight, *right panel*)) of C57BL/6 mice treated with Ex-4 or PBS for 4h-7 days. *n*=5 in each group. *** p<0.001 Ex-4 *vs* PBS. D) DNA content (*left panel*), protein content (*middle panel*) and DNA:protein ratio (*right panel*) per mg of pancreas tissue for mice treated with Ex-4 or PBS for 24h-7 days. *P < 0.05, ** p<0.01 Ex-4 vs PBS. (E-F) qPCR analysis of RNA from pancreata of mice treated for 4h-7 days (E) or 4 weeks (F). The levels of the indicated transcripts were determined by real-time PCR, normalized to cyclophilin (*Ppia*) mRNA content. Results are expressed as a fold difference relative to PBS and as means ± SE. *P < 0.05, ** p<0.01, p*** p<0.001 Ex-4 *vs* PBS n = 5 (E) or 10 (F) mice in each group.

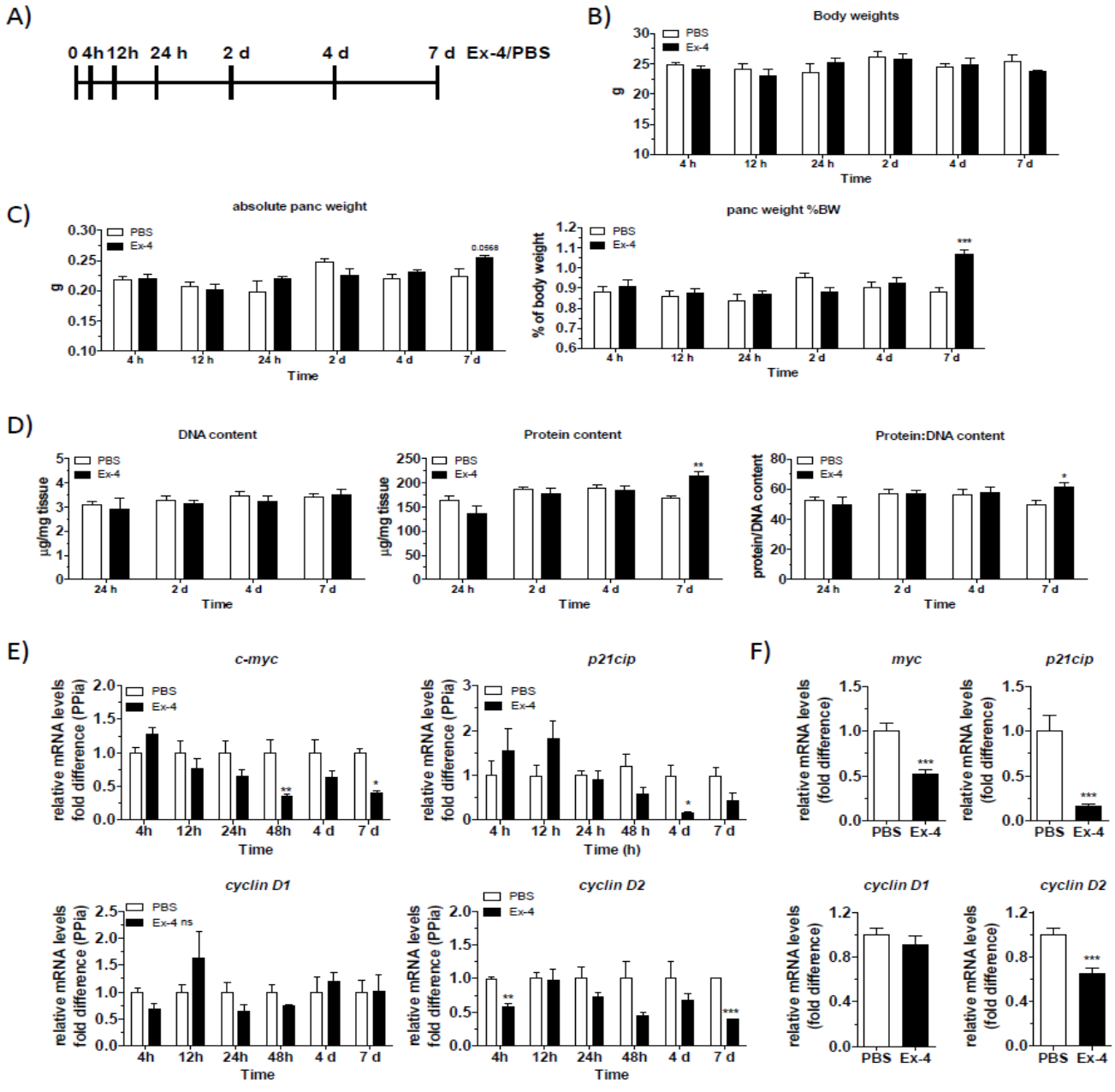

SUPPLEMENTARY DATA

Supplementary Figure 3. A) Body weights of mice administered Ex-4 or PBS with or without pretreatment with rapamycin (2 mg/kg 1x daily ip) over the course of the 7 day treatment as indicated. B) qPCR analysis of RNA isolated from the pancreas of the above treated mice. The levels of the indicated transcripts were determined by real-time PCR, normalized to cyclophilin (*Ppia*) mRNA content. Results are expressed as means ± SE. #$P < 0.05$, ## $p<0.01$ rapamycin *vs* vehicle. $n = 5$ male C57BL/6 mice in each group.

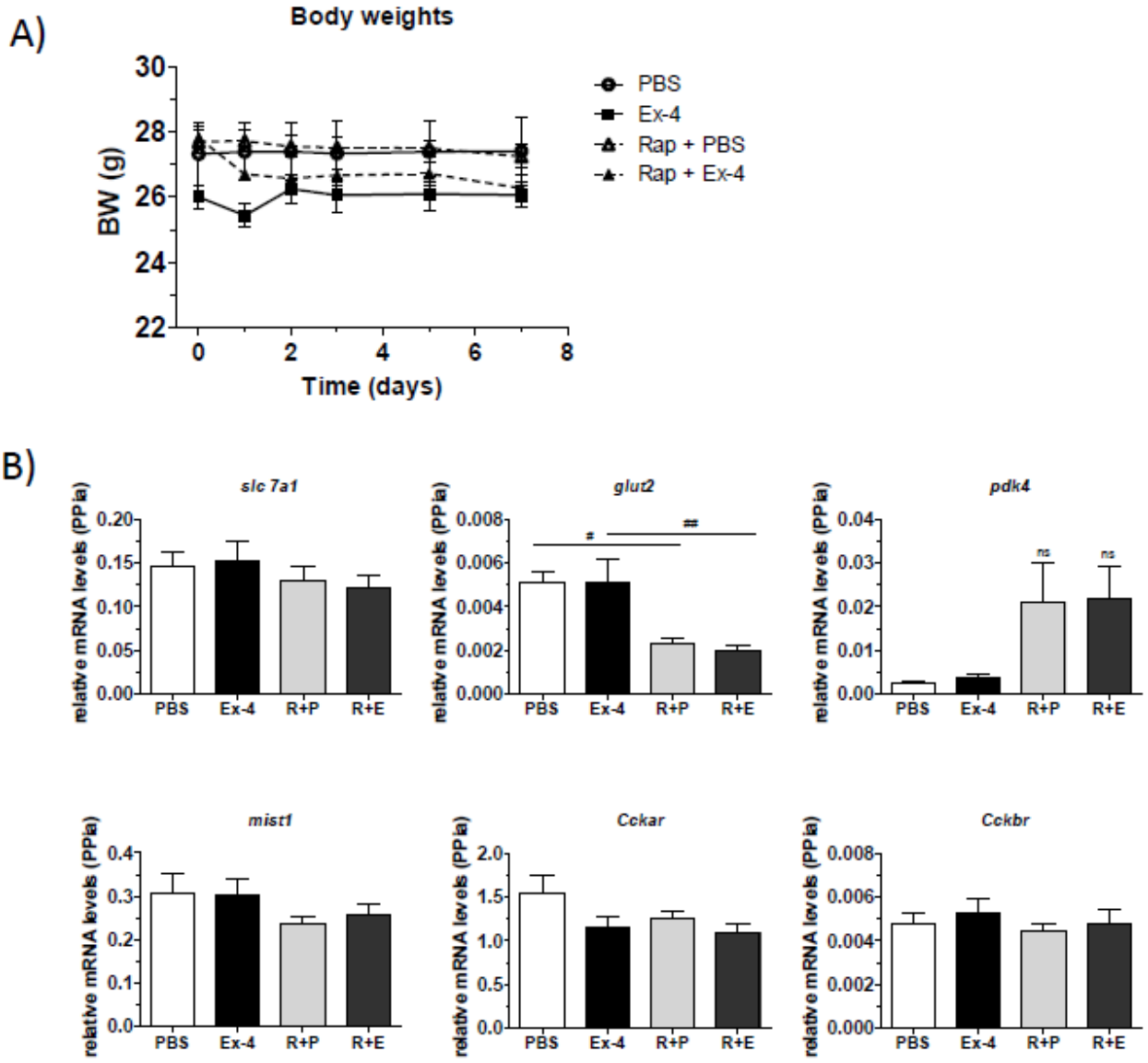

SUPPLEMENTARY DATA

Supplementary Figure 4. A-B) qPCR analysis of pancreatic RNA from mice treated with Ex-4 or PBS for 7 days (A), or 4 weeks (B). The levels of the indicated transcripts were determined by real-time PCR, normalized to cyclophilin (*Ppia*) mRNA content. Results are expressed as a fold difference relative to PBS an as means ± SE. **P* < 0.05, p*** p<0.001 Ex-4 *vs* PBS. *n* = 5 male C57BL/6 mice (A) or *n* = 12 male and female mice (B). C) qPCR analysis of RNA isolated from whole pancreas tissue or islets isolated from WT mice. The levels of the indicated transcripts were determined by real-time PCR, normalized to cyclophilin (*Ppia*) mRNA content. Results are expressed as means ± SE relative to whole pancreas tissue. *n* = 1 (whole pancreas, or islets isolated from 1 mouse).

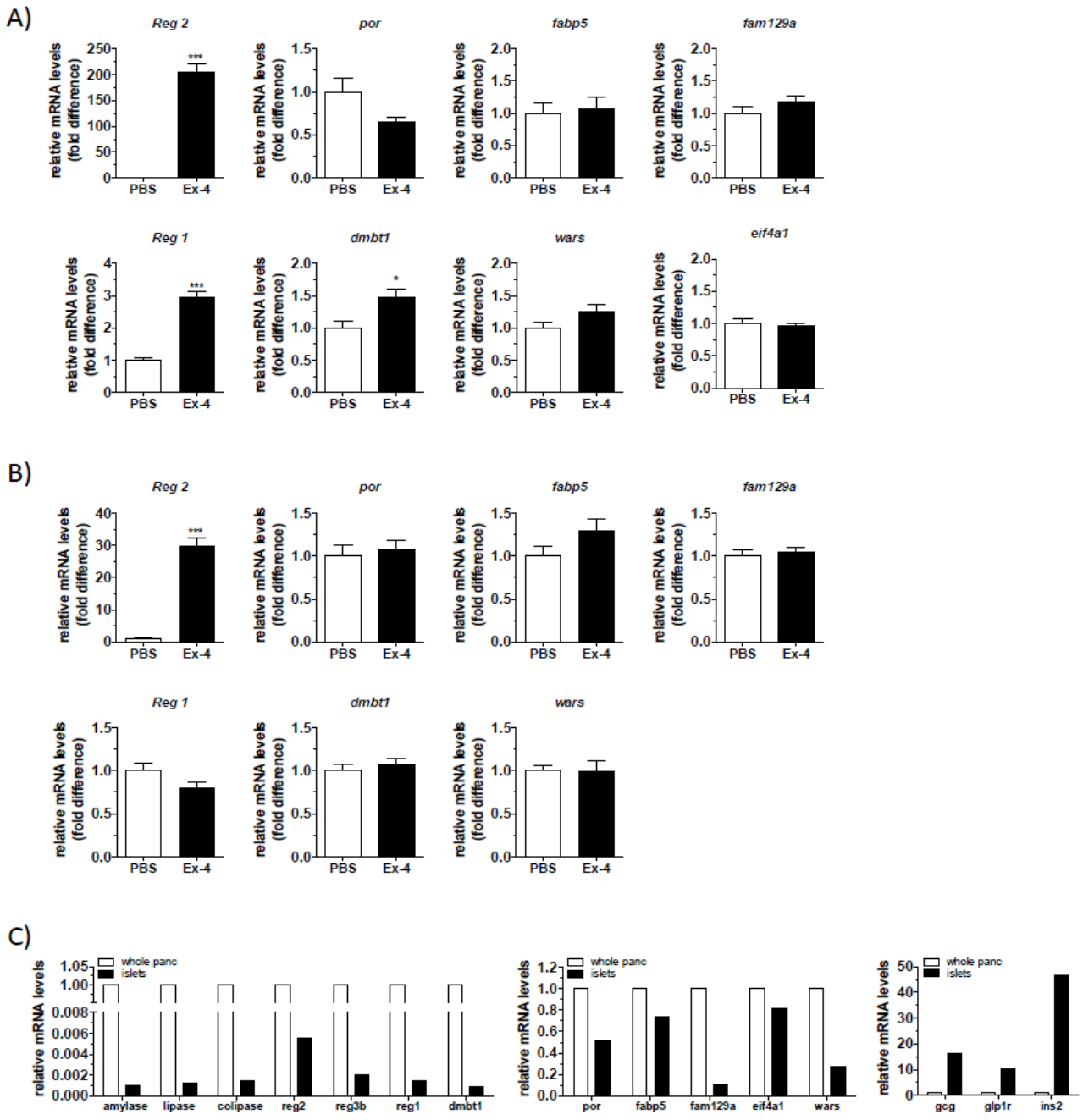

SUPPLEMENTARY DATA

Supplementary Figure 5. Immunohistochemical localization of Reg3 (A) and phospho-S6 (B) in the pancreas of mice treated with vehicle (PBS) or Ex-4 for 1 week (A) or Ex-4 for 3 days (B). Photomicrographs are representative of results detected in pancreata from four mice per group. Islets are represented with an *i*. Rare Reg3-immunopositive acinar cells in control (PBS) treated mice (A) or infrequent phospho-S6-immunopositive cells in islets (B) are indicated by the arrows. Magnification 400x (left panel) or digital enlargement of the area enclosed in the square.

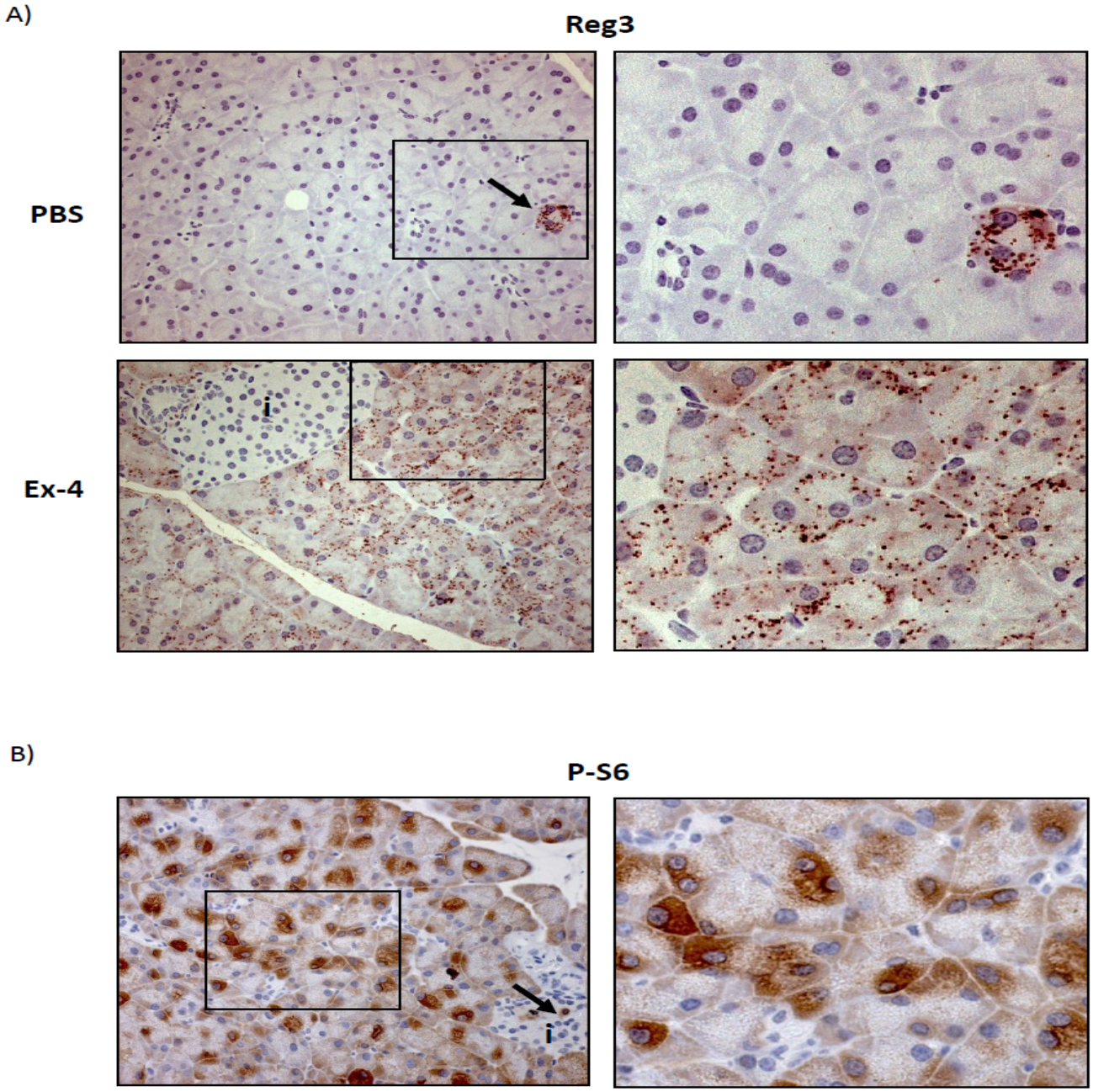

SUPPLEMENTARY DATA

Supplementary Table 1. Elucidation of the pancreatic proteome in mice treated with saline vs. exendin-4. Data from the proteomic analysis (Qspec analysis) of whole pancreas tissue from male C57BL/6 mice administered Ex-4 or vehicle (PBS) for 7 days. *n*=5 for control (PBS) and 4 for treatment (Ex-4). Shown is the protein ID, Gene ID, Gene name, individual spectral counts for each mouse (S1-S5, control (PBS): S6-S9, Ex-4 treatment), Log Fold Change Zstatistic, and False discovery rate (FDR). Log Fold Change values (natural log of estimated fold change) indicates the increase or decrease of protein concentration after 7 days, Zstatistic (Log Fold Change divided by the standard error of Log Fold Change) measures the statistical significance of the change, and False discovery rate (FDR) is the error rate estimated for a particular Zstatistic threshold calculated from the replicate data consistency and degree of change between control (PBS) and experimental (Ex-4) for each protein. Scale of 0-1 with 1 being random. Fold differences >2 and 5% or 0.05 fdr up or 0.05 fdr down was chosen as a cutoff for the summary data (Table 1).. FDRup: Global FDR for up-regulation in treatment (Ex-4) over control (PBS) treated mice. FDRdown: GlobalFDR for down-regulation in treatment over control. 2µg of digested sample was analyzed using nano-LC/MS with an Eksigent Ultra HPLC and a home-packed 75µm C18 column (Reprosil 3um C18). Buffer A was 0.1% formic acid in water; buffer B was 0.1% formic acid in ACN. The HPLC delivered an acetonitrile gradient over 230 min (2-35% buffer B over 180 min, 35-80% buffer B over 10 min, hold buffer B at 80% 10 min, and return to 2% B at 215min). The DDA parameters for acquisition on the TripleTOF 5600 were 1 MS scan (250ms; mass range 400-1250) followed by a) up to 20 MS/MS scans (100ms each). Candidate ions between 2-5 charge state and above a minimum threshold of 200 counts per second were isolated using a window of 0.7amu. Previous candidate ions were dynamically excluded for 20sec with a 50 mDa window. **Mass spectrometry data extraction:** Wiff files were converted to mzXML using AB Sciex MS Data Converter and ProteoWizard (3.0.4468; (1) and analyzed using the iProphet pipeline (2) implemented within ProHits (3) as follows. The database consisted of the mouse complements of the RefSeq protein database (version 53) supplemented with "common contaminants" from the Max Planck Institute (http://maxquant.org/downloads.htm) and the Global Proteome Machine (GPM; http://www.thegpm.org/crap/index.html). The search database consisted of forward and reversed sequences (labeled "DECOY"); in total 58202 entries were searched. The search engines used were Mascot (2.3.02; Matrix Science) and Comet (2012.01 rev.3; (4) with trypsin specificity (1 missed cleavages were allowed) , carbamidomethyl (C) was set as a fixed modification and deamidation (NQ) and oxidation (M) as variable modifications. Charges +2, +3 and +4 were allowed, and the parent mass tolerance was set at 30 ppm while the fragment bin tolerance was set at 0.15 amu. The resulting Comet and Mascot search results were individually processed by PeptideProphet (5) and combined into a final iProphet output using the Trans-Proteomic Pipeline (Linux version, v0.0 Development trunk rev 0, Build 201303061711). TPP options were as follows: general options are -p0.05 -x20 -PPM -d"DECOY", iProphet options are –ipPRIME and PeptideProphet options are –OpdP. All proteins with a minimal iProphet probability of 0.95 were exported and processed with the QSPEC program. This corresponded to 1959 proteins at an estimated FDR of ~1%. The QSPEC program (6) was used to identify differential protein abundance between pancreas samples from Ex-4 and PBS (control) treated mice by statistical analysis of spectral count data exported from iProphet. QSPEC reports log fold change, Zstatistic and false discovery ratios (FDR) for fold change data for each protein.

SUPPLEMENTARY DATA

Supplementary Table 2. Summary of proteomics data for amylase and lipase –related proteins, and islet-associated proteins. Log fold change represents the overall change in pancreas protein after 7 days of treatment. Zstatistic reports a combined value of the confidence and fold change data. Individual fdr values for fold changes as reported by the Qspec algorithm.

References

1. Kessner D, Chambers M, Burke R, Agus D, Mallick P. ProteoWizard: open source software for rapid proteomics tools development. *Bioinformatics* 2008;**24**:2534-2536
2. Shteynberg D, Deutsch EW, Lam H, et al. iProphet: multi-level integrative analysis of shotgun proteomic data improves peptide and protein identification rates and error estimates. *Molecular & cellular proteomics : MCP* 2011;**10**:M111 007690
3. Liu G, Zhang J, Larsen B, et al. ProHits: integrated software for mass spectrometry-based interaction proteomics. *Nature biotechnology* 2010;**28**:1015-1017
4. Eng JK, Jahan TA, Hoopmann MR. Comet: an open-source MS/MS sequence database search tool. *Proteomics* 2013;**13**:22-24
5. Keller A, Nesvizhskii AI, Kolker E, Aebersold R. Empirical statistical model to estimate the accuracy of peptide identifications made by MS/MS and database search. *Anal. Chem* 2002;74:5383-5392
6. Choi H, Fermin D, Nesvizhskii AI. Significance analysis of spectral count data in label-free shotgun proteomics. *Molecular & cellular proteomics : MCP* 2008;**7**:2373-2385